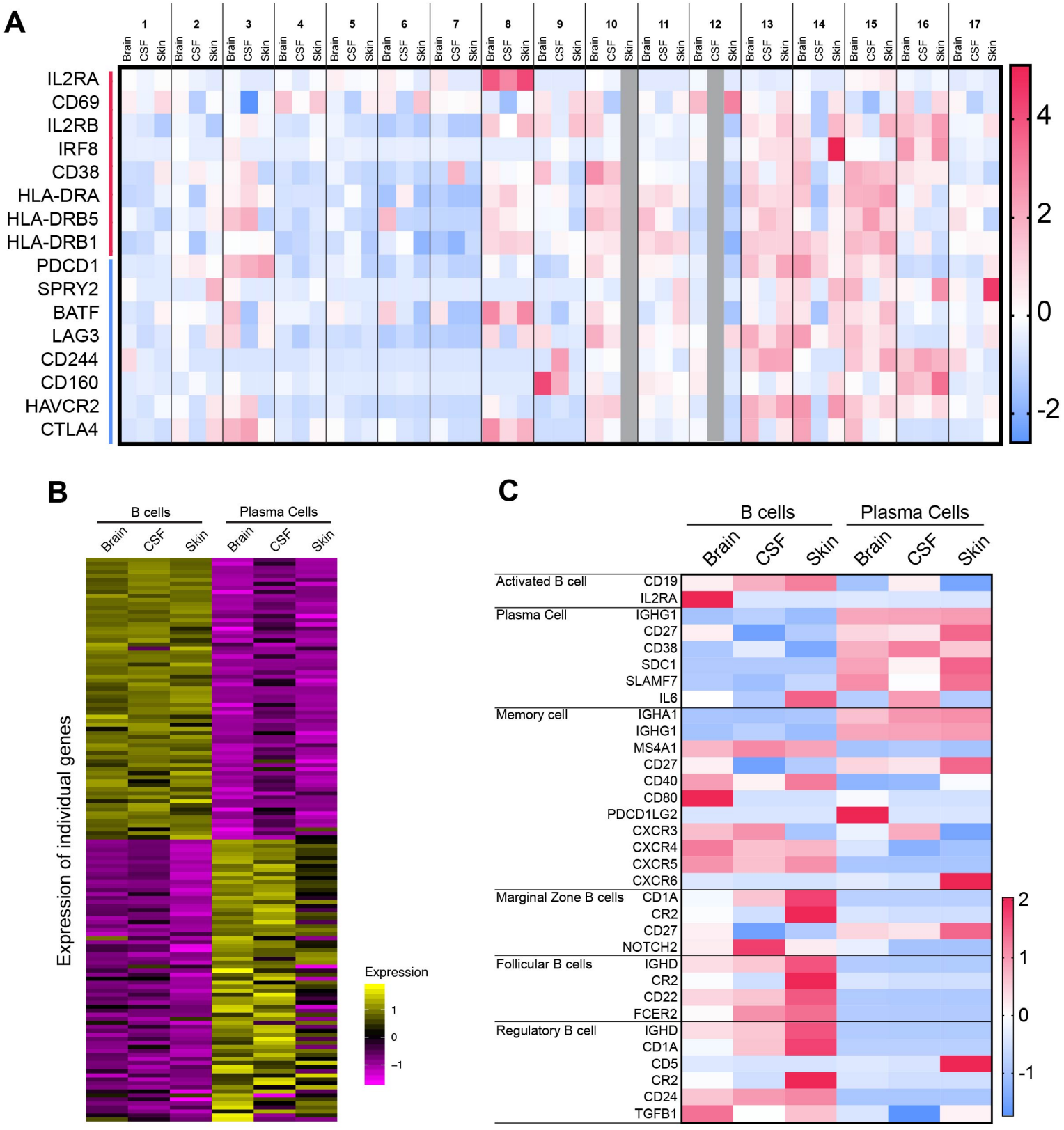

Supplemental Figure 1. A. Expression of T and NK cell activation markers and immune checkpoints by metastatic site. **B.** Gene expression profiles of B cells and plasma cells across all samples. **C.** Heatmap showing B cell and plasma cell markers across metastatic sites.

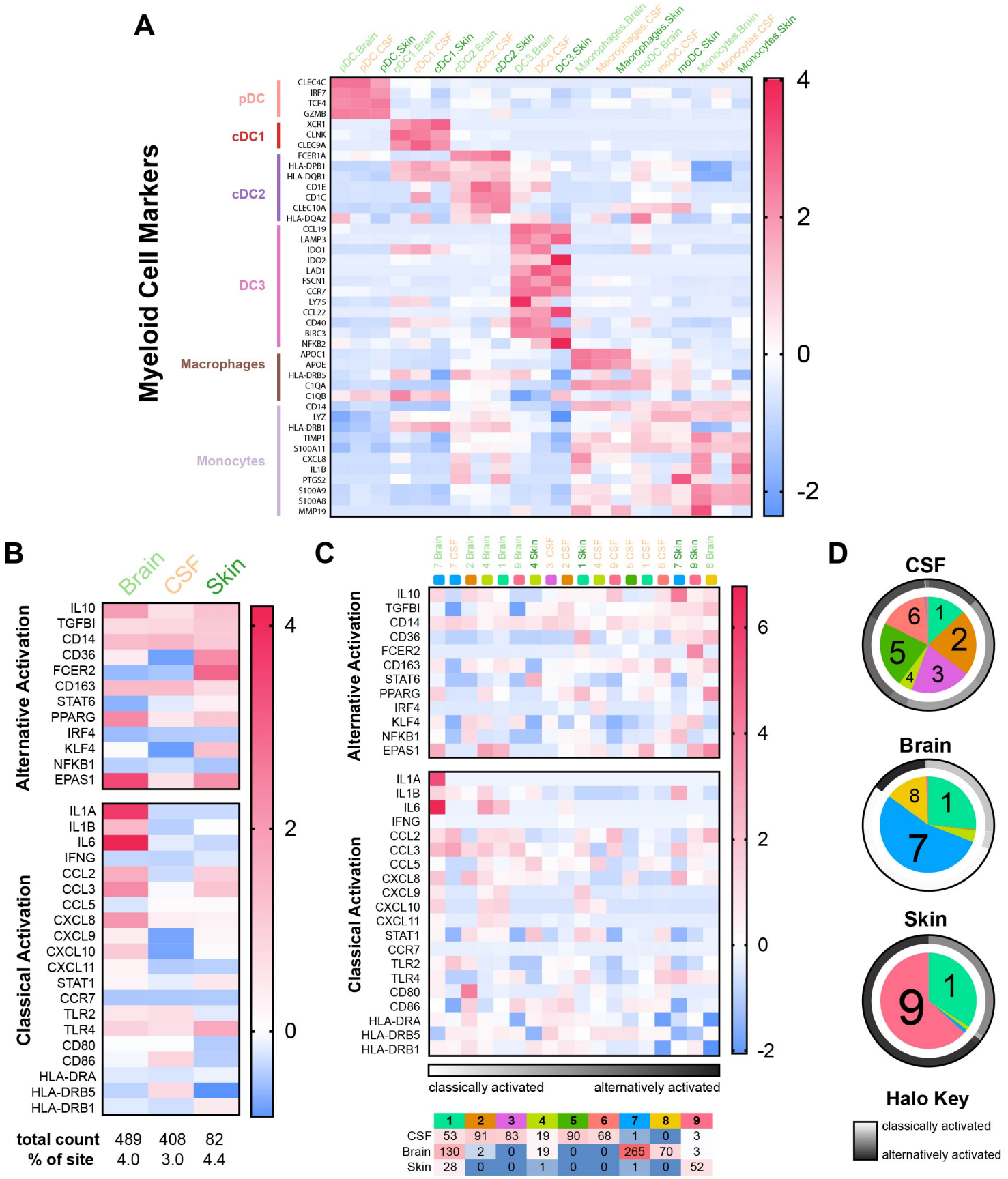

Supplemental Figure 2. A. Expression of myeloid cell markers by metastatic site. **B.** Gene expression associated with classical and alternative macrophage activation in all macrophages by site of metastasis. **C.** Gene expression associated with classical and alternative macrophage activation in nine individual macrophage subpopulations by site of metastasis (top). Distribution of macrophage subpopulations by total cell counts of individual sub-clusters across metastatic sites (bottom). **D.** Pie charts show macrophage composition by metastatic site. Colored halo indicates predicted activation program of each macrophage sub-cluster based on gene expression profiles specific to respective metastatic site.

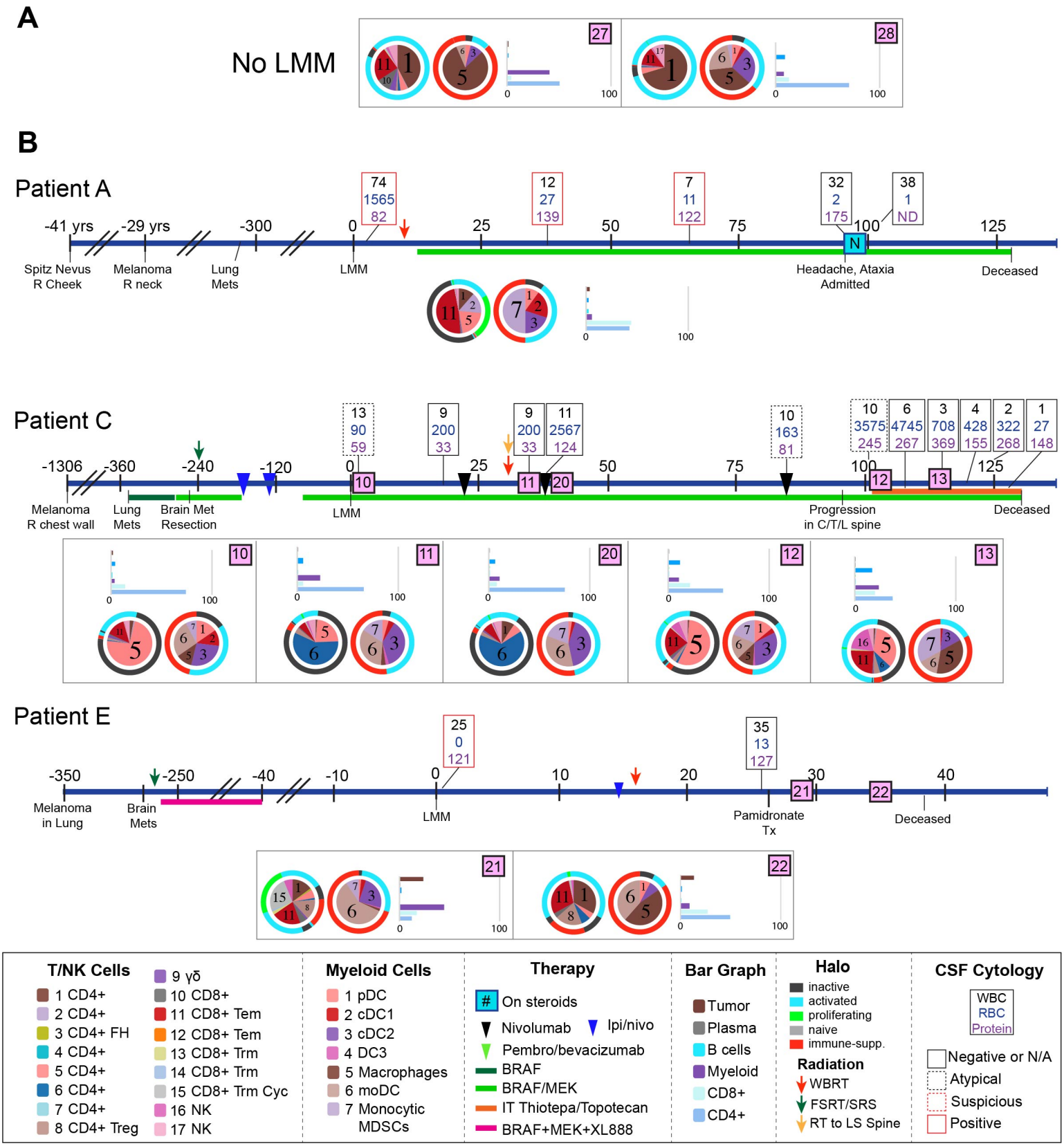

Supplemental Figure 3. A. Snapshots of each control sample from patients without metastasis to the central nervous system, with pie charts showing the cellular landscape for T cells (left pie chart) and myeloid cells (right pie chart). Halo indicates predicted behavior of each cell sub-cluster (e.g. inactive, activated, proliferating, naïve and immune suppressive). Bar graph shows percent of tumor made up of tumor cells, plasma, B cells, myeloid cells and CD4+ or CD8+ T cells. **B-E.** Treatment timeline of two poor responders, with accompanying cellular landscape information as panel A, showing much greater proportion of T cell compartment to be comprised of inactive T cell sub-classes and a greater portion of the myeloid cell compartment to be comprised of immune-suppressive cell sub-classes than the exceptional responder in Figure 4D.

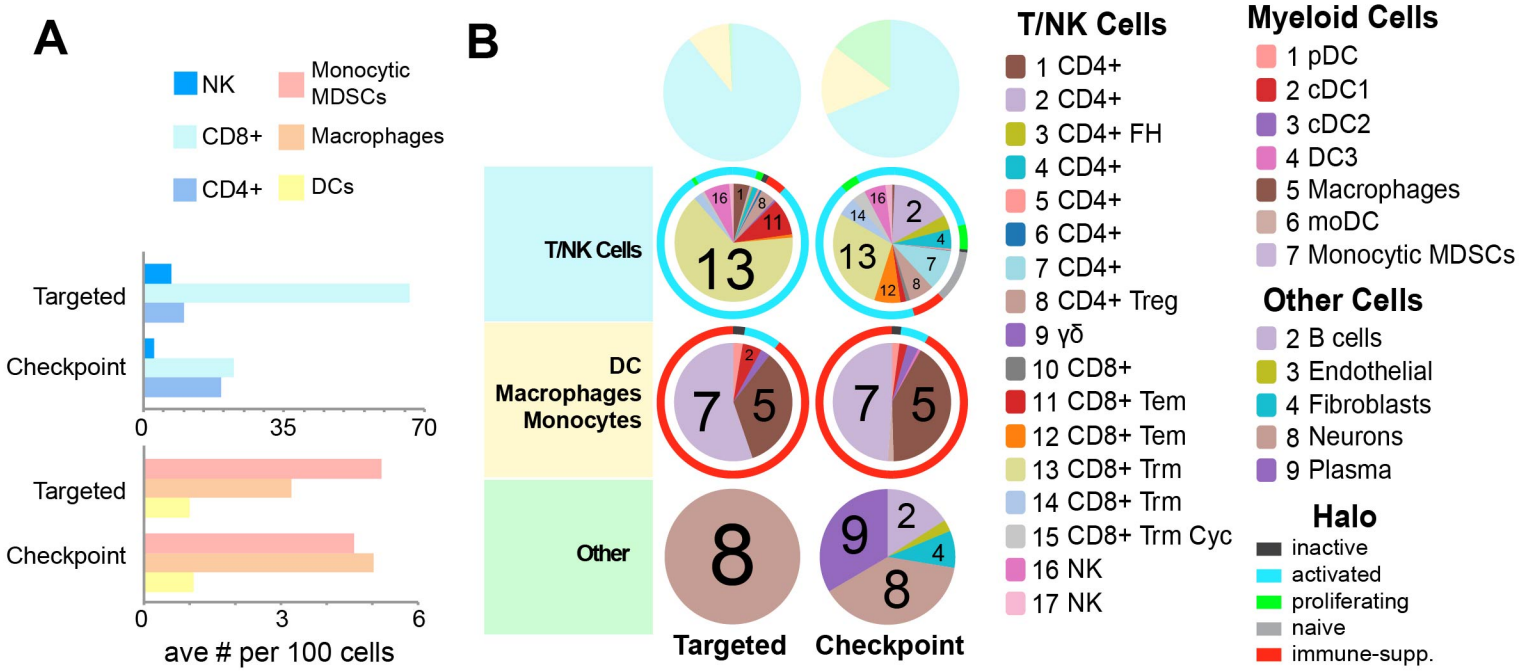

Supplemental Figure 4. A. Cell type distribution of brain metastasis samples treated with targeted therapy or immunotherapy, breakdown by major lymphocytic and myeloid cell types, normalized to every 100 cells analyzed. **B**. Detailed breakdown of cell phenotypes for T/NK cells, myeloid cells and other cells. Halo indicates predicted behavior of each cell sub-cluster (e.g. inactive, activated, proliferating, naïve and immune suppressive).

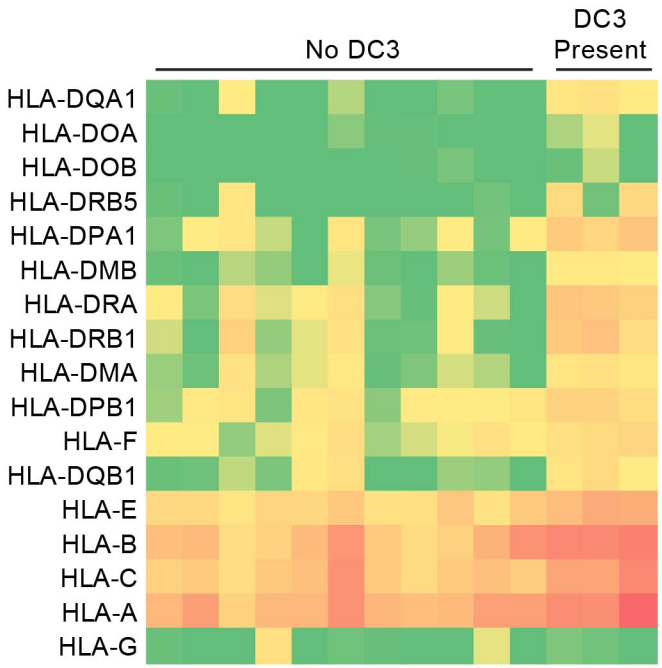

Supplemental Figure 5. Heatmap showing relative expression of MHC class I and II molecules on melanoma cells from samples with and without DC3 present.

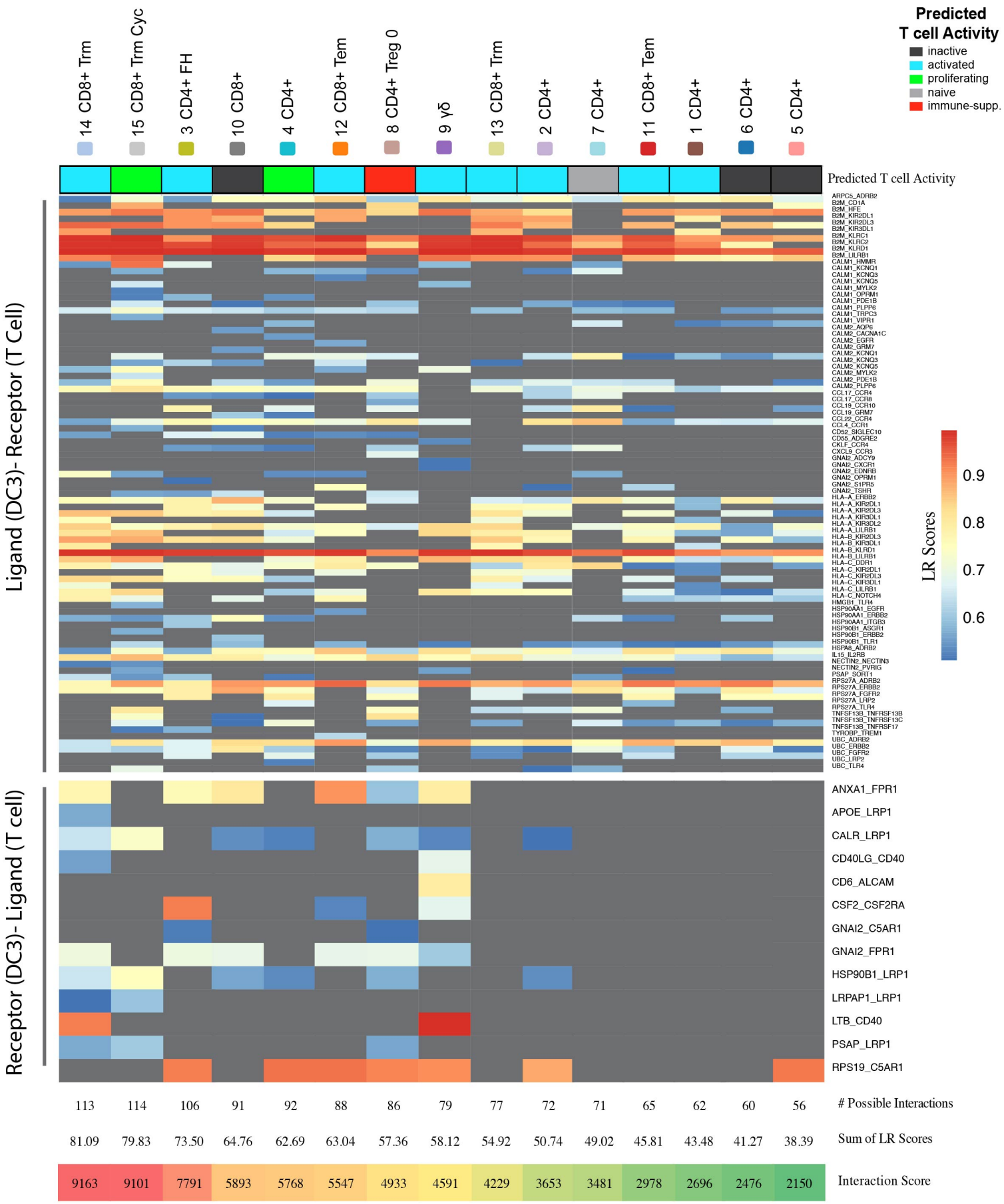

Supplemental Figure 6. Cell-cell interaction analysis using SingleCellSignalR. Heatmap visualizing the interactions with LRscore higher than 0.5 between DC3 and CD4 or CD8 subpopulations, further filtered by DC3-specific markers. The interaction score is a product of the number of all interactions with LRscore higher than 0.5 and the sum of these interactions' LR scores.

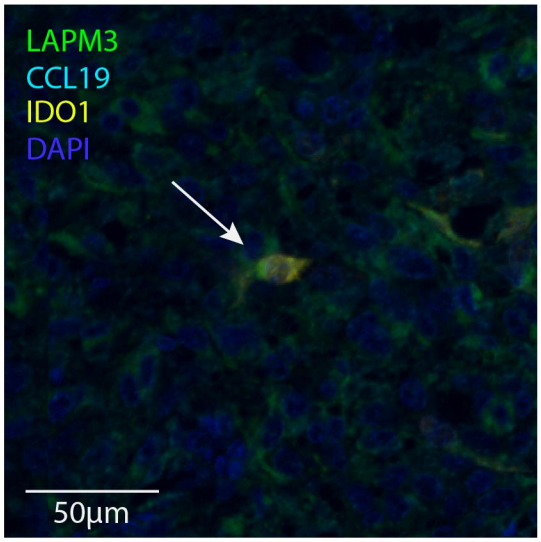

Supplemental Figure 7. Multiplex-IF staining for DC3 cells using DAPI (blue), LAMP3 (green), CCL19 (cyan) and IDO1 (yellow). Representative image showing detection of a DC3 cell in MB-15 sample.

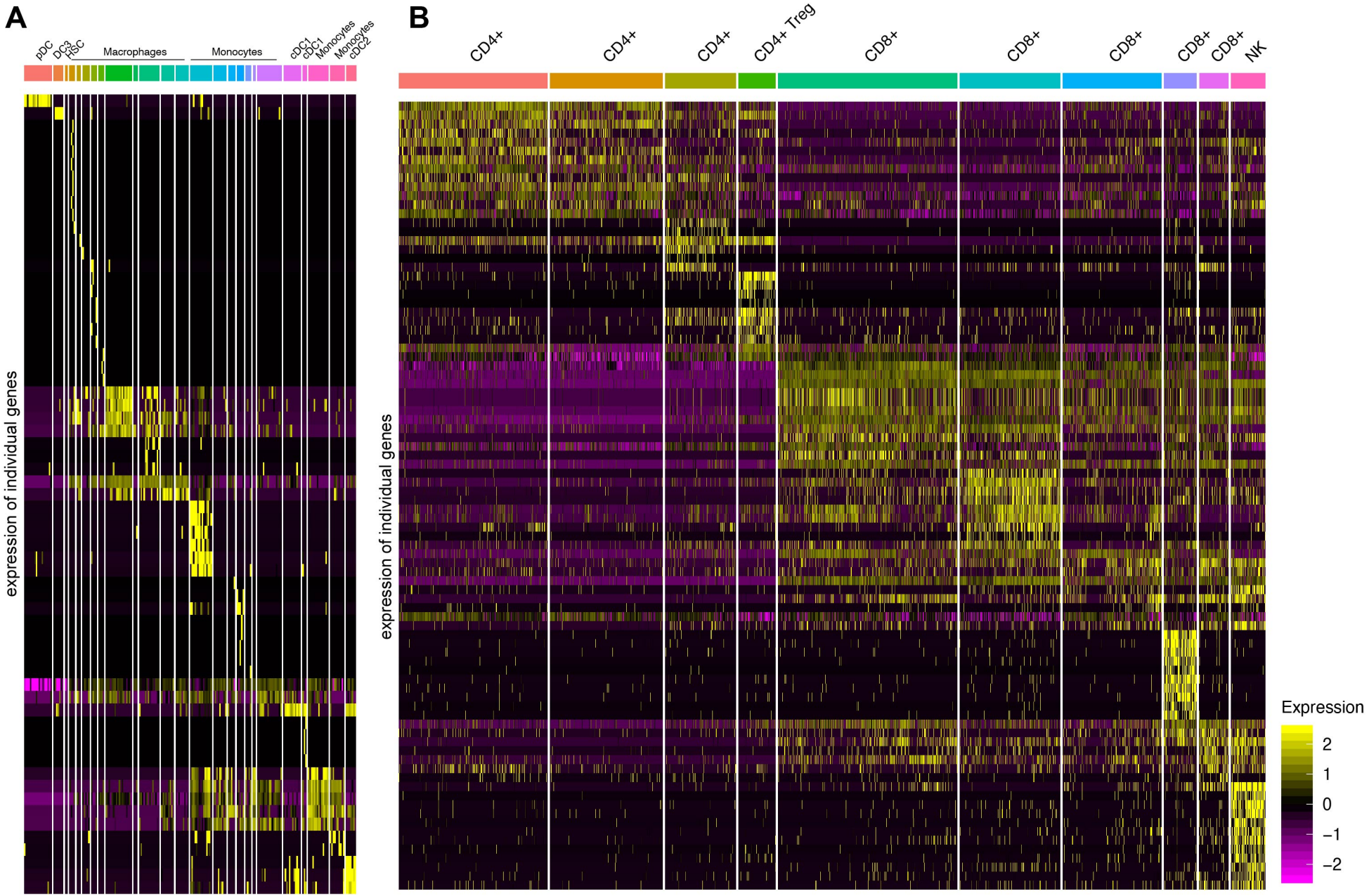

Supplemental Figure 8. Validation analysis of samples from melanoma metastases in a publicly available validation dataset (Tirosh et al, 2016). **A.** Unsupervised clustering identified the 25 myeloid cell clusters. **B.** Unsupervised clustering identifies 9 subsets of T cells and 1 cluster of NK cells.

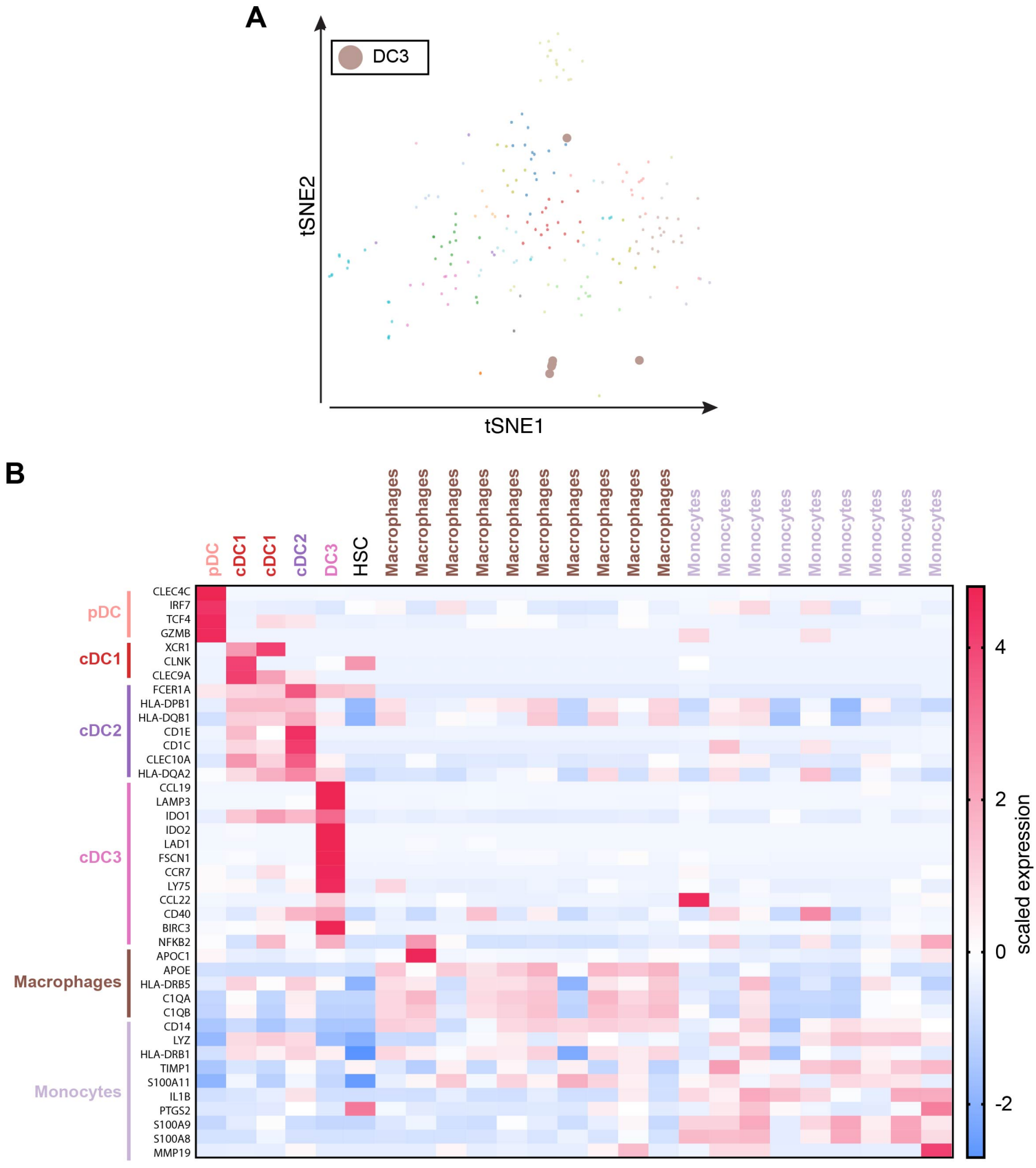

Supplemental Figure 9. A. t-SNE plot showing the distribution of myeloid cells in melanoma samples from a publicly available validation dataset (Tirosh et al, 2016). The DC3 cells are highlighted in larger brown circles. **B.** Expression of key markers that distinguish the major subsets of myeloid cells, including DC3, in validation dataset.

A

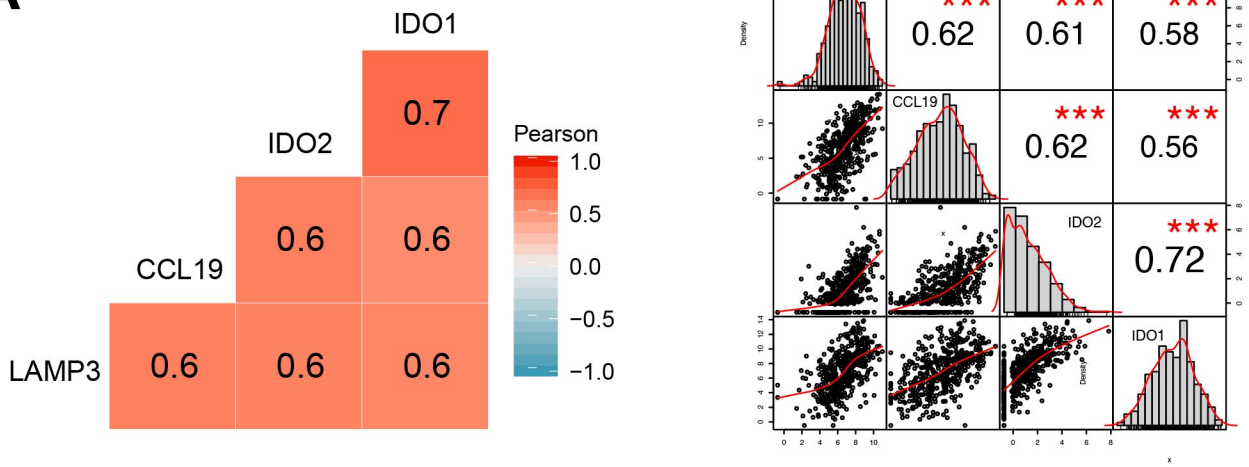

B

	PC1	PC2	PC3	PC4
CCL19	0.49	-0.54	-0.66	0.20
IDO1	0.50	0.59	0.07	0.62
IDO2	0.52	0.37	-0.14	-0.76
LAMP3	0.49	-0.47	0.73	-0.03

C

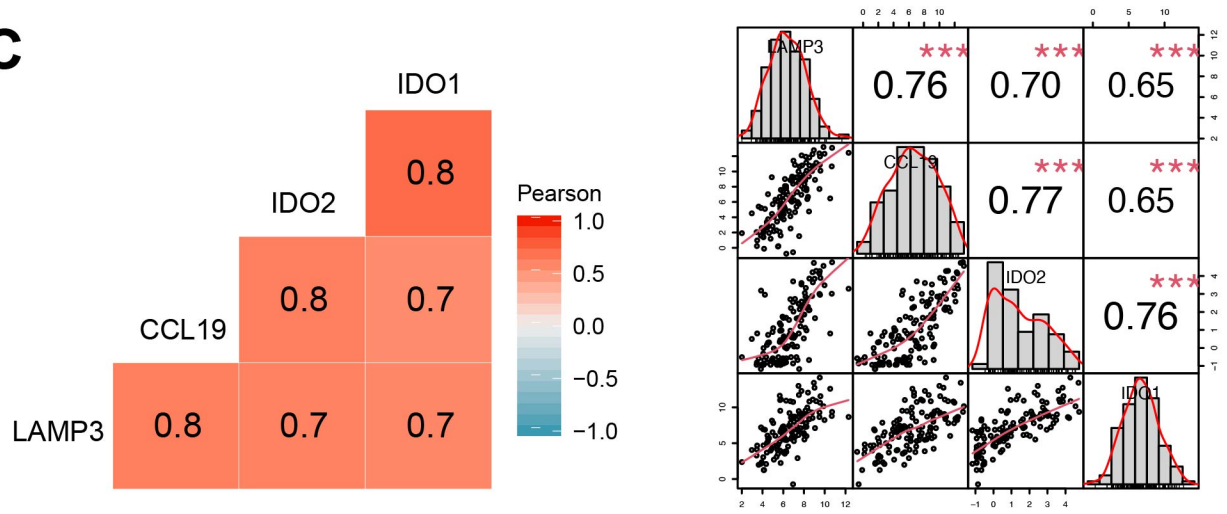

Supplemental Figure 10. A. Correlation of DC3 gene signature in TCGA. **B.** PC loading for DC3 gene signature in TCGA. **C.** Correlation of DC3 gene signature in Moffitt Cohort (N=135).

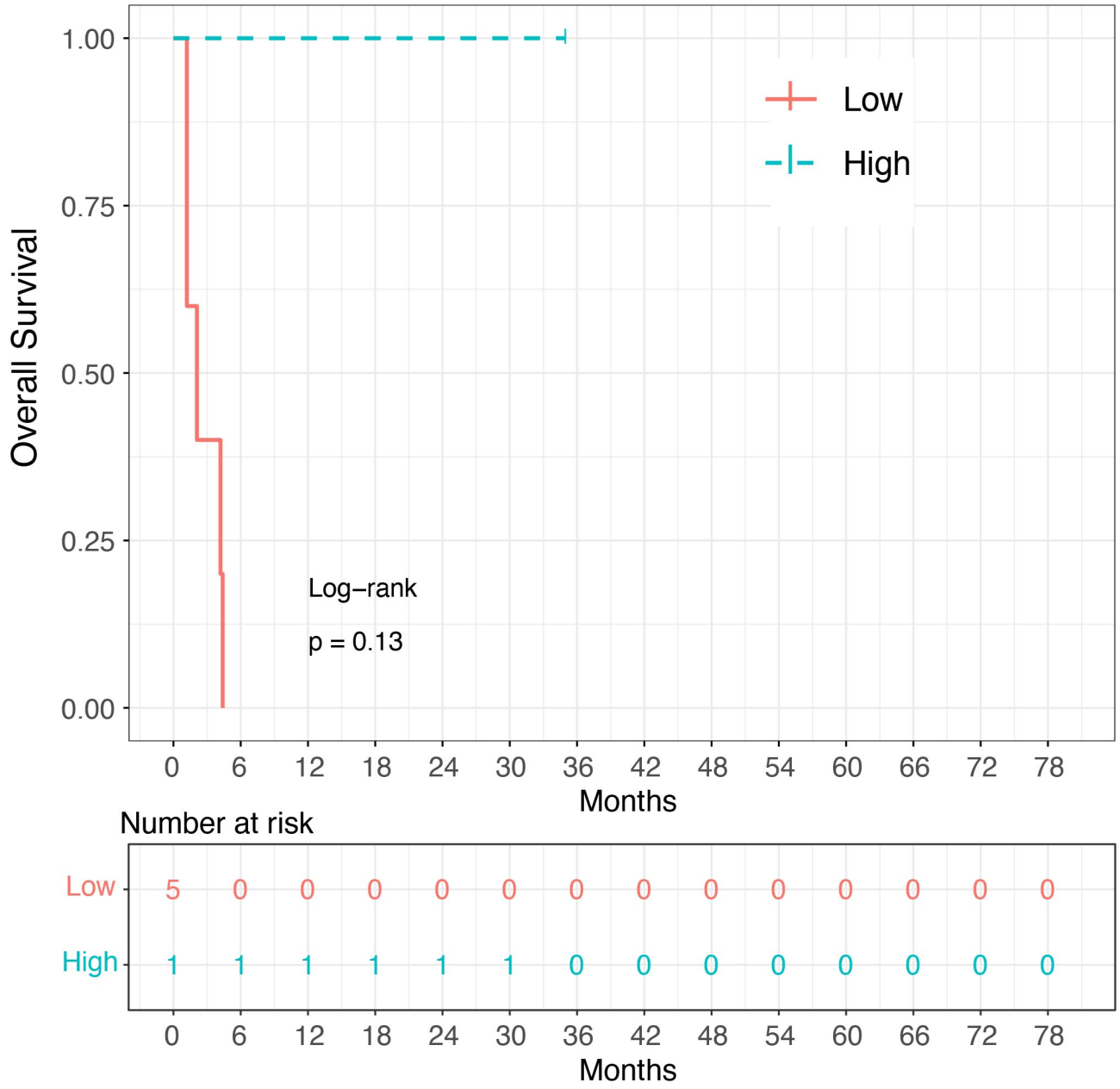

Supplemental Figure 11. Overall survival for melanoma patients with LMM metastases whose CSF samples contained high DC3 cells vs. low DC3 cells (cut point 0.45).

A

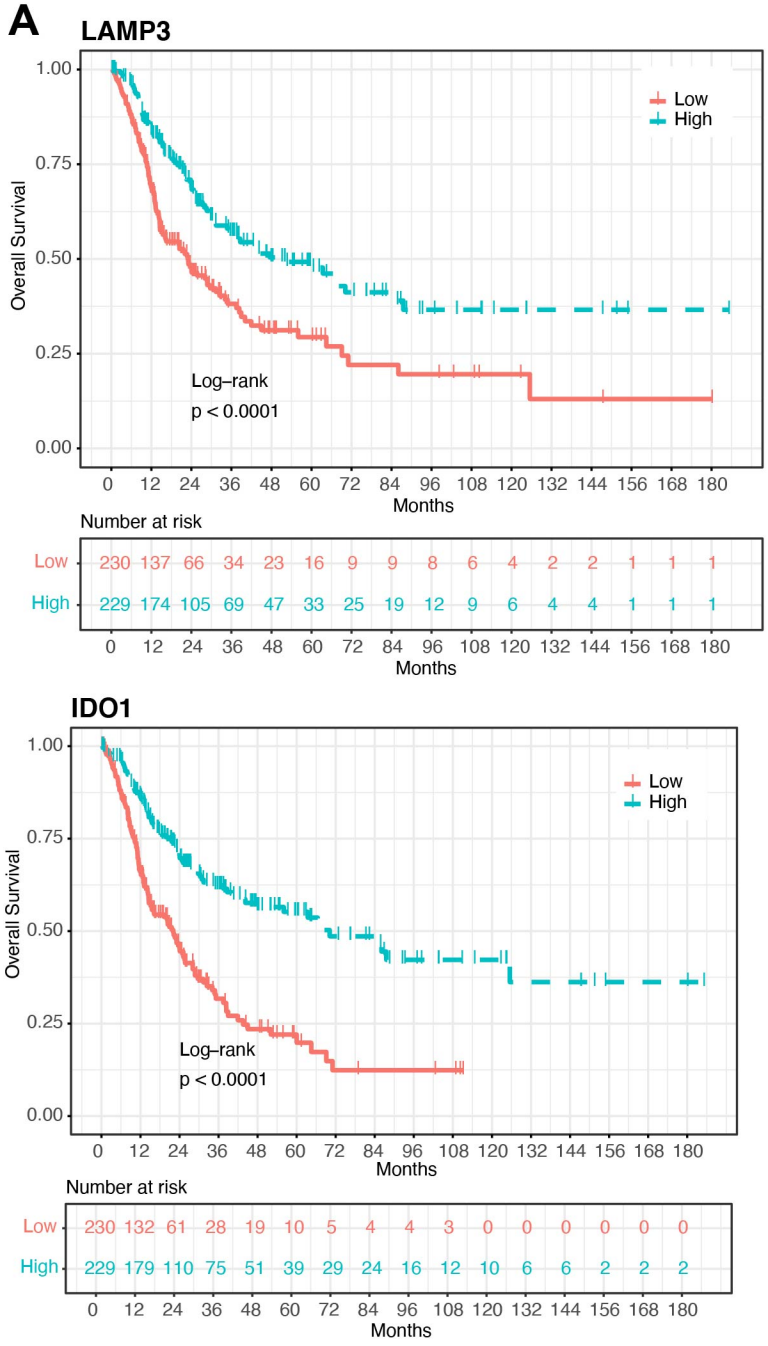

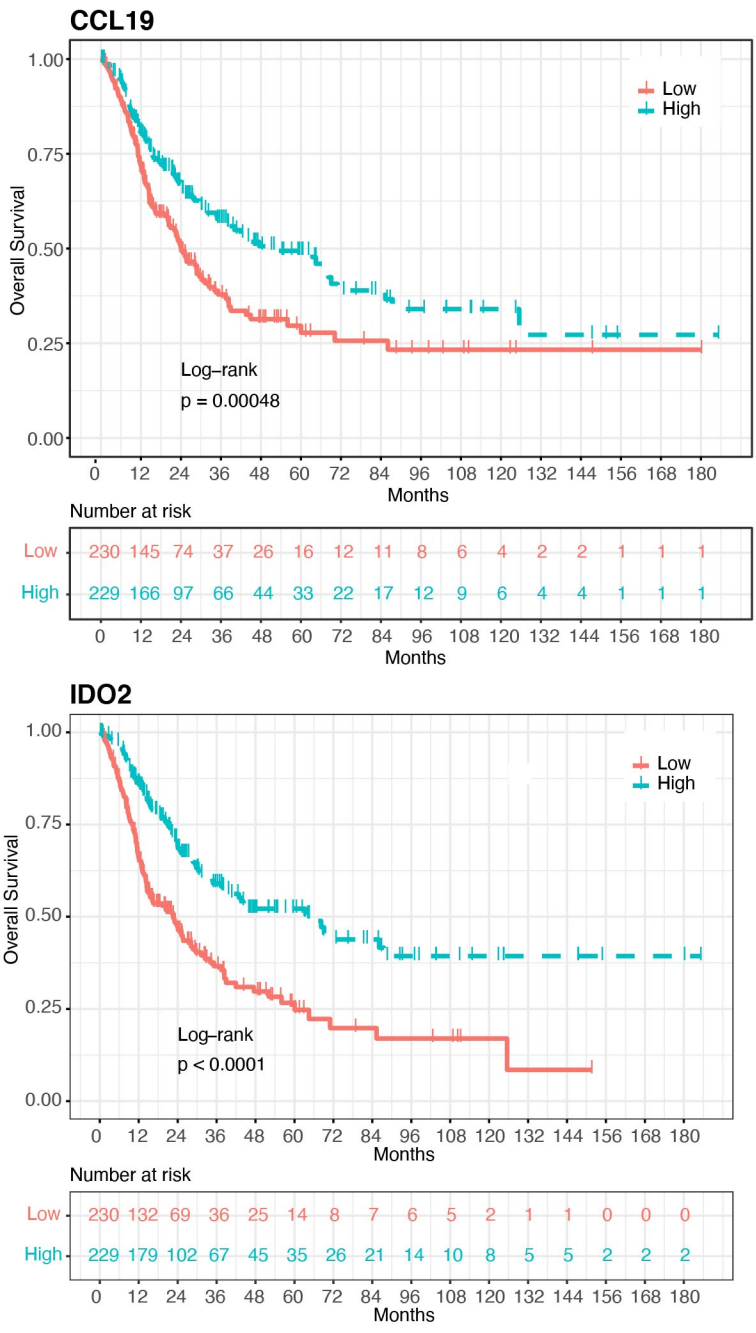

B

Variable	HR	p_value	HR_95CI
LAMP3	0.83	0.00000006862	0.78 ~ 0.89
CCL19	0.92	0.00004347	0.89 ~ 0.96
IDO2	0.76	0.000000006346	0.69 ~ 0.83
IDO1	0.86	0.00000000008922	0.82 ~ 0.9
PC1	0.77	0.0000000001332	0.71 ~ 0.83

Supplemental Figure 12. A. Correlation of individual genes from the DC3 gene signature to overall survival in TCGA dataset. **B.** Univariate cox proportional-hazards models for individual genes from the cDC3 gene signature in TCGA dataset.